

# One CHiP to rule them all? Mechanistic insight into carfilzomib-induced lung injury with neutrophil extracellular trap formation following cellular immunotherapy

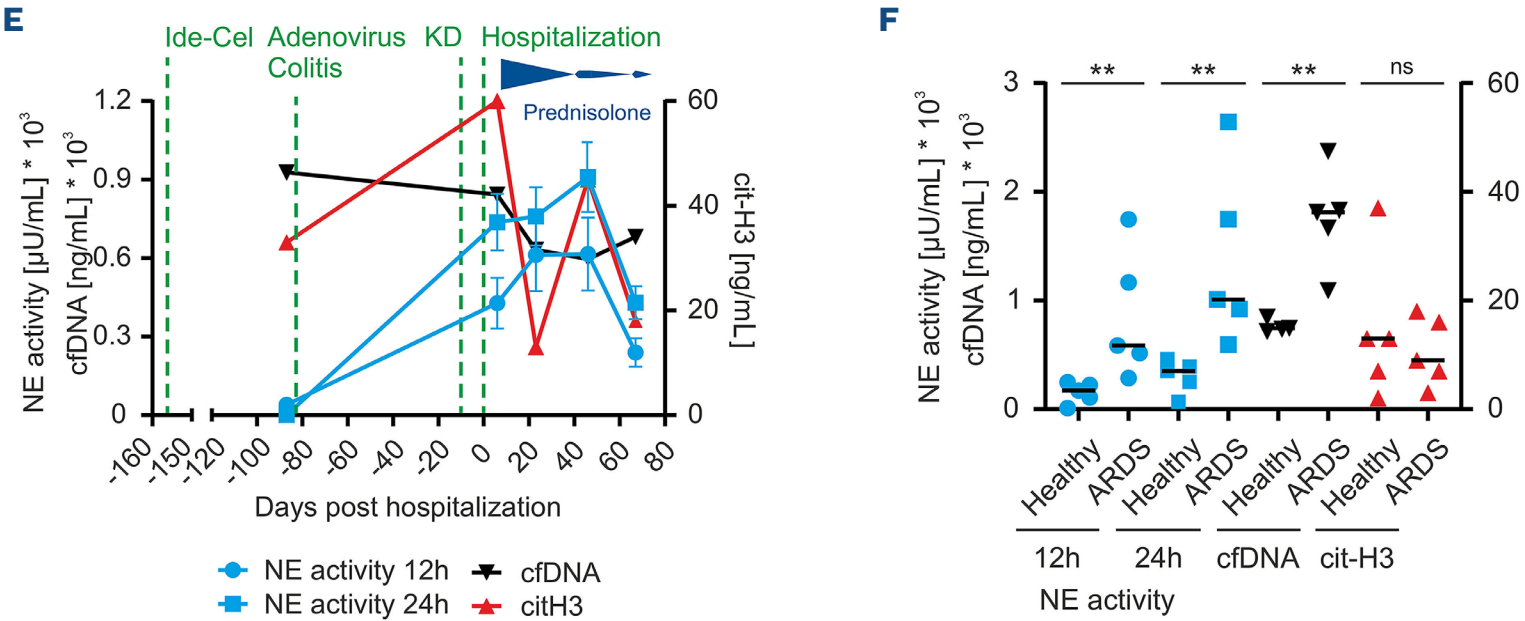
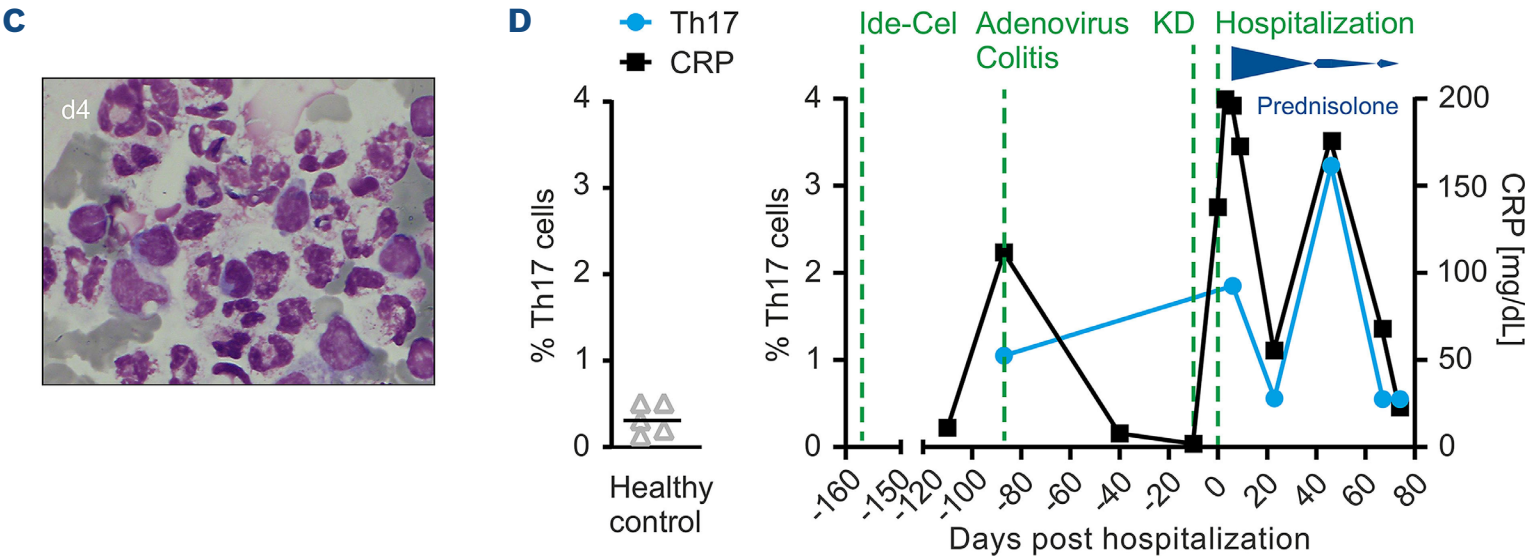
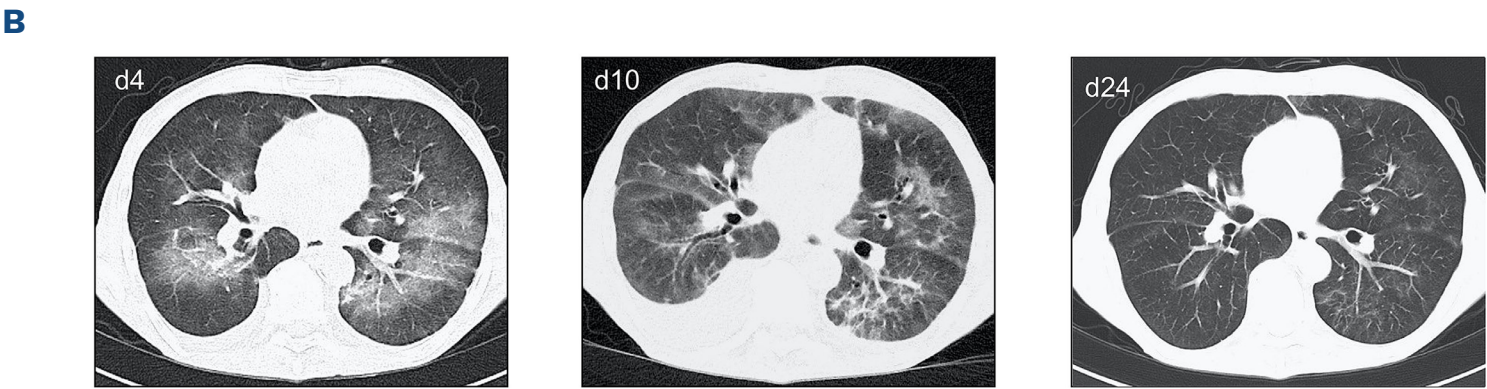
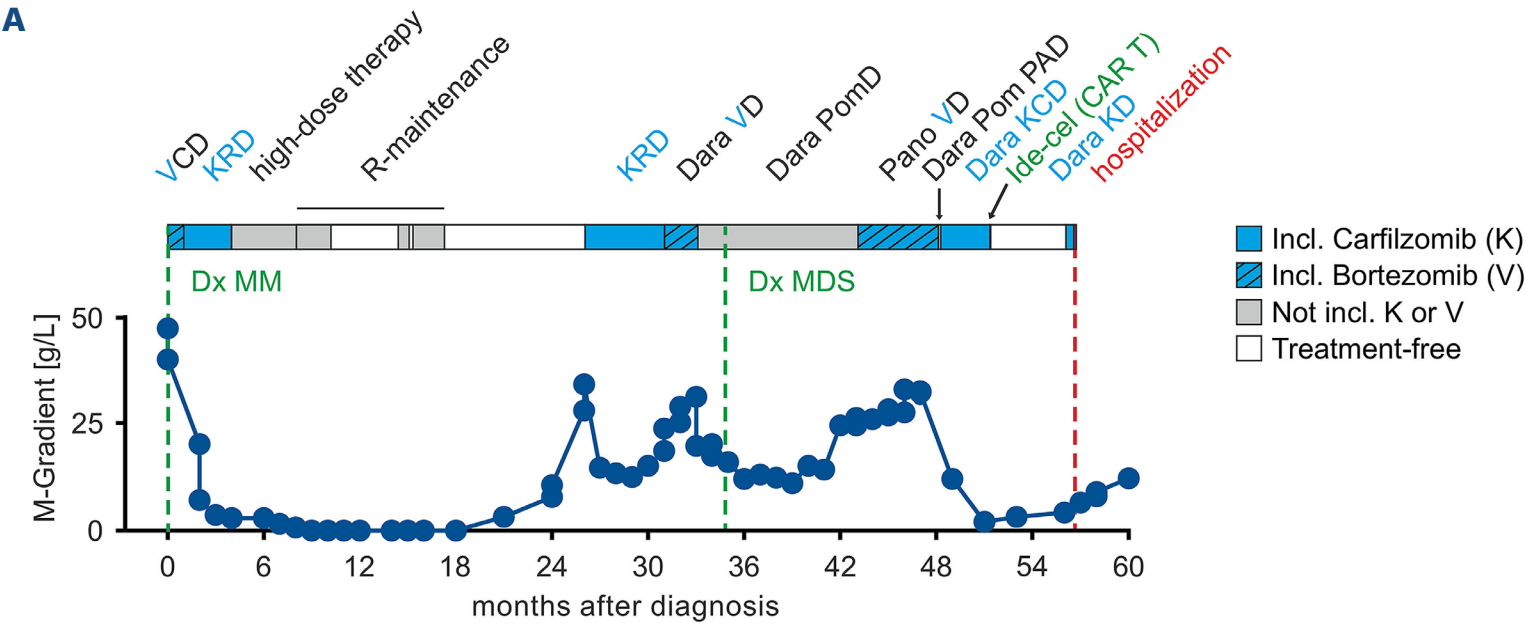
Multiple drugs can trigger drug-induced lung injury (DILI).<sup>1</sup> DILI is diagnosed after excluding cardiac, infectious or malignant differential diagnoses.<sup>1</sup> Patients show non-specific clinical symptoms like cough, fever, dyspnea and hypoxemia. In severe cases, DILI can lead to respiratory failure and acute respiratory distress syndrome (ARDS).<sup>1</sup> Typical radiographic manifestations are bilateral ground glass opacities (GGO) in several lobes with or without consolidations.<sup>1</sup>

Proteasome inhibitors (PI) are effective against multiple myeloma (MM). The PI bortezomib and carfilzomib inhibit the proteasome highly selectively in a reversible and irreversible manner, respectively.<sup>2</sup> Both PI reportedly induce DILI as a rare side effect with variable kinetics.<sup>3-5</sup> Typically, DILI occurs after several doses of the respective PI. For bortezomib, the mean time from the first application to onset of symptoms is 31 days (range, 1-336 days) and usually occurs 1 to 32 days after the last dose.<sup>6</sup>

We report on a 78-year-old male patient with MM type IgG $\lambda$  who received multiple therapy regimes including high-dose melphalan and autologous stem cell transplantation, lenalidomide maintenance, bortezomib- or carfilzomib-containing regimens, and several other lines (Figure 1A). Blood samples including controls were obtained with written informed consent (Ethics' approval numbers #513-20, #193\_13B, #174\_20B, 19-336\_1B). At month 35 after treatment initiation, a poorly resolving cytopenia prompted a bone marrow puncture and identified morphologic alterations typical for myelodysplastic syndrome (MDS). At month 51, the 9<sup>th</sup> line of therapy with B-cell maturation antigen (BCMA)-directed chimeric antigen receptor (CAR) T cells ide-cel achieved partial remission. Progressive disease was detected only 5 months after ide-cel infusion. The patient was then re-exposed to daratumumab (16 mg/kg, day 1), carfilzomib (36 mg/m<sup>2</sup>, days 1/2, 8/9, 15/16) and dexamethasone (20 mg days 1/2, 8/9, 15/16). Ten days after the first post-CAR T application of carfilzomib and 1 day after the last dose (day 9), the patient developed high fever of up to 39.7 °C, tachypnoea and tachycardia (pulse 110/minute [min], respiratory rate 41/min, peripheral oxygen saturation 93 %). In venous blood gas analysis, pO<sub>2</sub> was decreased (17.7 mmHg) and pCO<sub>2</sub> was normal (43.2 mmHg) suggesting partial respiratory insufficiency. C-reactive protein (CRP) was elevated at 138 mg/L. High-resolution computer tomography (HR-CT) of the thorax revealed bilateral GGO in the central sites and lower lobes, consolidation in intermediate lobe and unilateral

pleural effusion (Figure 1B). The patient was hospitalized (day 1) and received broad-spectrum antibiotics to address suspected infectious pneumonia. However, dyspnea and hypoxia worsened, high fever persisted, and CRP further increased to 215 mg/L. Blood cultures remained negative, Epstein-Barr virus (EBV) and Cytomegalovirus (CMV) reactivation as typical complication following BCMA-CAR T-cell therapy were excluded by polymerase chain reaction (PCR) testing. By bronchoscopy, the mucosa appeared normal and mucosal secretions were clear. Broad bacterial, mycobacterial, fungal, and viral PCR-diagnostics from bronchoalveolar lavage (BAL) remained negative. Microscopic differentiation of the hypercellular BAL showed over 80% neutrophils, an elevated fraction of erythrocytes and only few alveolar macrophages and lymphocytes (Figure 1C). The high number of neutrophils triggered empirical escalation of the broad-spectrum antibiotics. However, respiratory insufficiency worsened and high infection parameters persisted. Day 10 HR-CT revealed progression of basal GGO, of interstitial infiltrates and of pleural effusions (Figure 1B). The lack of other differential diagnoses prompted the diagnosis of DILI. One hundred mg of prednisolone daily were initiated from day 10. Within 2 days, oxygen insufflation was stopped, CRP decreased quickly, and clinical conditions improved enabling a discharge from the hospital only 4 days after starting the steroids (Figure 1D). With step-wise tapering of prednisolone, GGO and pleural effusion in chest HR-CT resolved by day 24.

After reviewing patient's medication prior to DILI, carfilzomib was the only reasonable suspicion of causing DILI. Most important treatment approaches to proteasome inhibitor (PI)-induced DILI are high-dose glucocorticoids and end of drug exposure.<sup>1</sup> Typical corticosteroid therapy regimens to induce remission are high-dose methylprednisolone (1 mg/kg body weight) or dexamethasone (40 mg) for 1 to 4 days followed by tapering.<sup>1</sup> Steroid-refractory cases typically have fatal prognosis.<sup>1</sup> Acute PI-induced pulmonary toxicity is suspected to be mediated by toxic drug products and appears rapidly after the very first dose.<sup>7</sup> In contrast, delayed reactions after multiple PI doses are typical of immune reactions and are usually responsive to steroids. The few reported carfilzomib-induced cases of DILI showed onset between a few hours (h) and up to 24 h after administration of the most recent carfilzomib dose; this is similar to our case which started less than 24 h after infusion.<sup>3,5</sup>



Continued on following page.



**Figure 1. Linking carfilzomib-induced drug induced lung injury to neutrophil extracellular trap formation.** (A) Overview of therapies and corresponding M-gradient over time from first diagnosis of multiple myeloma (MM). (B) Computer tomography scans of similar lung sections showing ground glass opacities at day 2 and (Dx) 10 and improvement after a 2-week steroid administration at day 24. (C) Bronchoalveolar lavage (BAL) accomplished at day 8 showing a predominantly neutrophilic infiltrate. (D) Concentration of IL-17A producing CD4<sup>+</sup> T cells (Th17) of healthy donors and of our patient over time in correlation to the level of C-reactive protein in patient's serum. Th17 cells were measured after intracellular staining by flow cytometry, each symbol represents one individual measurement. C-reactive protein (CRP) was determined in clinical routine testing. (E) Activity of neutrophil extracellular trap (NET) formation was determined over-time by determining neutrophil elastase (NE) activity and levels of cit-H3 in the patient serum by quantitative enzyme-linked immunosorbent assay from serum. (F) NE activity and cit-H3 were measured from healthy individuals or from severe acute respiratory syndrome Coronavirus 2-(SARS-CoV-2) patients in acute respiratory distress syndrome as described in (E). Each symbol represents an individual patient. Two-group comparison was done using the Mann Whitney test; d: day.

Clinical presentation as well as CT-findings of our case also matched the described pattern.

In our patient, the disease pattern reflected features of severe ARDS<sup>8</sup> or of severe acute respiratory syndrome Coronavirus 2 (SARS-CoV-2) pneumonia where neutrophilic lung inflammation has been associated with formation of neutrophilic extracellular traps (NET).<sup>9</sup> Current understanding of NET-formation suggests activation of neutrophils in reactive oxygen (ROS) and/or Calcium<sup>2+</sup>-dependent pathways.<sup>10</sup> Intracellular proteins are citrullinated by peptidyl arginine deiminase 4 (PAD4). Specifically, citrullination of histone H3 (cit-H3) leads to decondensation of the chromatin which then is ejected into the extracellular space.<sup>11</sup> Neutrophil elastase (NE), which in homeostasis is rapidly inactivated in the blood by abundant  $\alpha$ 1-antitrypsin, is protected by NET from inactivation. In addition, NET-bound PAD4 locally citrullinates and inactivates  $\alpha$ 1-antitrypsin. Consequently, active NE is present longer in the peripheral blood of patients with severe inflammation, even if the NET formation has already ended. We determined circulating NET-degradation products in the peripheral blood using the fluorogenic substrate MeOSuc-AAPV-AMC (Santa Cruz Biotechnology, Dallas, TX, USA) to assess the activity of NE in the serum. The mean fluorescence intensity (MFI) was recorded using the Tecan Infinite 200 Pro (Tecan, Männedorf, Schweiz) with 360 nm excitation and 465 nm emission for 24 h in 20 min intervals. Elastase from human leukocytes (Sigma-Aldrich, St. Louis, MO, USA) was used as standard to calculate the activity in  $\mu$ U/mL. Cell-free DNA (cfDNA) was detected using the Quant-iT<sup>TM</sup> PicoGreen<sup>TM</sup> dsDNA Assay-Kit (Thermo Fisher Scientific, Waltham, MA, USA) according to manufacturer's instructions. The concentration of citrullinated histone 3 (cit-H3) in serum was measured using the Citrullinated Histone H3 (Clone 11D3) ELISA Kit (Cayman Chemical Company, Ann Arbor, MI, USA) according to manufacturer's instructions. Cit-H3 and activity of NE were at normal levels 86 days prior to and substantially increased at hospitalization (day 0; Figure 1E). Despite the clinically effective steroid treatment, NE activity only gradually decreased in our patient in line with its protection when bound to NET. At the peak of DILI, NE activity was in the same range as in severe ARDS following SARS-CoV-2 infection (Figure 1F). In parallel to steroid-induced clinical

and CT-graphic resolution of inflammation, cit-H3 quickly normalized suggesting resolution of NET neogenesis. Neutrophilic inflammation frequently is associated with high C-reactive protein (CRP) and with elevated Th17 cells. To measure Th17 cells, cells were treated with PMA (2  $\mu$ g/mL)/Ionomycin (1  $\mu$ M) in the presence of Golgi Stop for 4 hours and stained with antibodies against surface proteins, washed, fixed and permeabilized with Cytofix/Cytoperm Kit (BD Biosciences, Heidelberg, Germany) and stained with an antibody against IL-17A (BD Biosciences, Heidelberg, Germany). Analyzed on an LSR Fortessa (BD Bioscience, Heidelberg, Germany), lymphocytes were determined by FSC-A/SSC-A, doublets (by FSC-A/FSC-H), dead cells (by 7-AAD) and monocytes (by CD14) were excluded, and cells were gated by the indicated monoclonal antibodies (mAb) with Kaluza software v2.1 (Beckmann Coulter, Krefeld, Germany). Our patient showed an increased rate of 1.05% Th17 cells with moderately elevated CRP at day -86 in an episode of adenovirus-associated colitis when compared with healthy controls (average rate 0.3% Th17 cells). Th17 cells further increased to 1.85% in DILI at hospitalization suggesting Th17-driven inflammation during the period of vascular NET formation (Figure 1D). Several days after steroid administration, levels of Th17 cells normalized. Despite good initial response, a likely too aggressive tapering led to a second, still steroid-sensitive episode of DILI. The second episode of DILI also showed steroid-reactive CRP, reduction of Th17 cells and cit-H3. The typical pattern of biomarkers of vascular NET, together with the high rate of Th17 cells and their responsiveness to steroids highlights a possible relation of the immune changes and DILI in the patient. After DILI was controlled, MDS progression was diagnosed at month 31. In line, increasing cytopenia was paralleled by increased blast counts in the bone marrow. Due to the progressive MDS, MM could not reasonably be treated any longer prompting initiation of best supportive care. The patient succumbed more than 7 months after diagnosis of DILI.

DILI described here was associated with neutrophil activation and NET formation. However, multiple carfilzomib-containing regimens were infused without lung toxicity before day 0 suggesting a change before the last cycle of carfilzomib. The progressive MDS coincided with the time

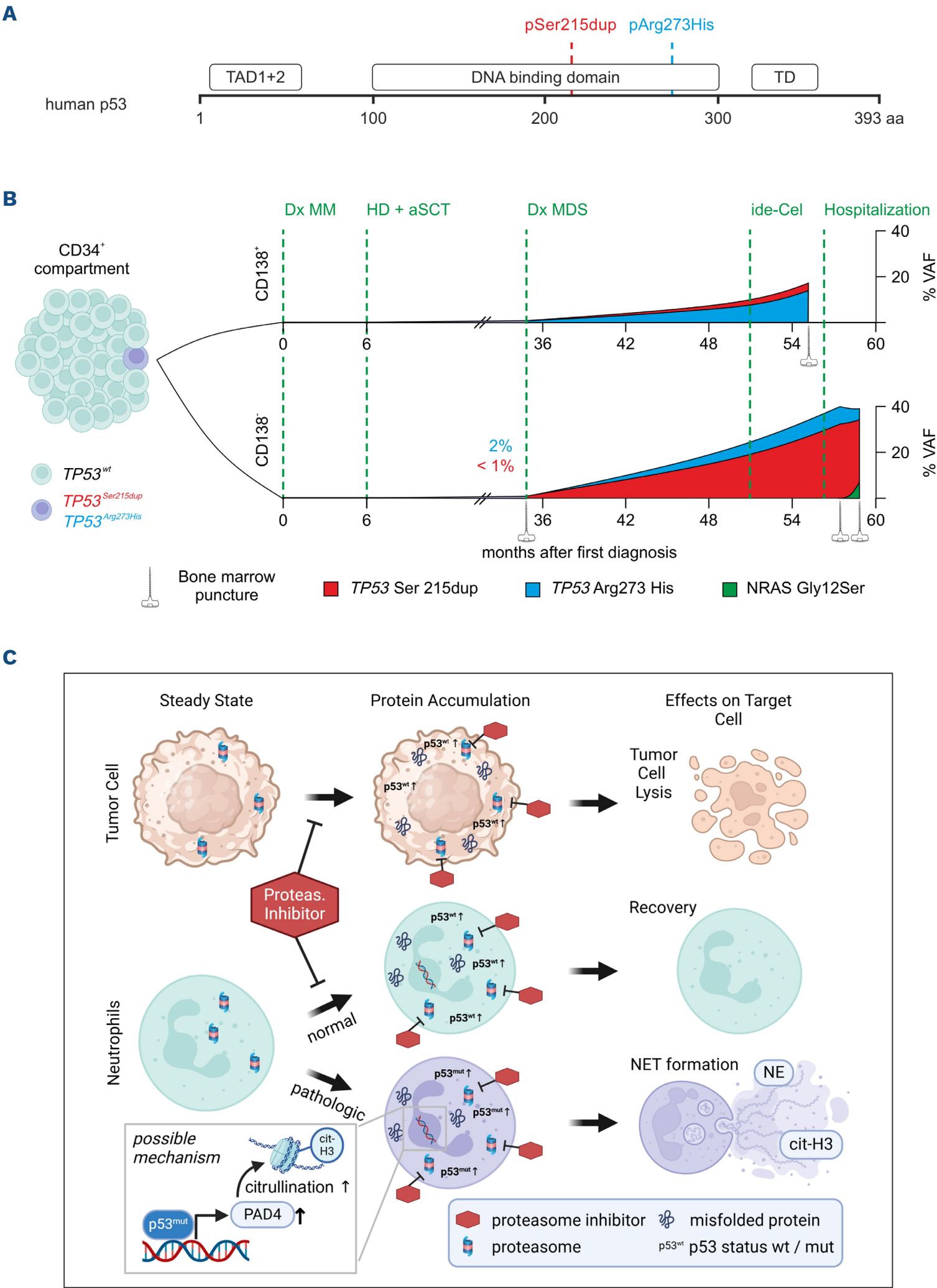


**Figure 2 Clonal evolution and neutrophil extracellular trap formation in drug induced lung injury.** (A) Patient’s *TP53* mutations are located in the deoxyribonucleic acid binding domain of p53. (B) Clonal evolution of *TP53* mutations in myelodysplastic syndromes (MDS) and multiple myeloma (MM). (C) Schematic model: proteasome inhibition leads to an increase of p53 protein. While in p53 wild-type (wt) neutrophils no disturbance occurs, the patient’s p53 mutations possibly lead to peptidyl arginine deiminase 4 (PADI4) induction leading to a citrullination of histones and induction of neutrophil extracellular trap (NET) formation. Created with BioRender.com. Dx: diagnosis; auto-SCT: autologous stem cell transplantation; VAF: variant allele frequency; NE: neutrophil elastase; cit-H3: citrullinated histone H3 elastase; cit-H3: citrullinated histone H3.

of carfilzomib toxicity. Mutations in the CD138<sup>+</sup> and CD138<sup>-</sup> bone marrow cells were analyzed by targeted sequencing on an illumine platform (MLL diagnostics laboratory, Munich) and showed an increased variant allele frequency (VAF) of the two mutations Arg273His and Ser215dup of the DNA binding domain of *TP53* (Figure 2A). Interestingly, the very same two mutations were present in both diseases and increased independently over the therapy lines to a maximum VAF of 40% in the MDS clone and 17% in the MM clone (Figure 2B). The joint mutation is most likely explained by a common CD34<sup>+</sup> ancestor for both diseases with similar clonal evolution under therapeutic pressure.

While Arg273His changes binding affinities to target genes,<sup>12</sup> alterations around Ser215 reduce phosphorylation by Aurora kinase B, which marks *TP53* for homeostatic degradation.<sup>13</sup> Consequently, Ser215dup enhances p53 protein stability and serves as gain-of-function mutation. One of the many transcriptionally regulated proteins of p53 is PAD4, which is crucial for the initiation of NET-formation (Figure 2C).<sup>14</sup> With the two *TP53* mutations at a VAF close to 50% in the CD34<sup>+</sup> cells, almost every peripheral neutrophil harbored one mutated *TP53* allele. Based on the clone data and literature, we speculate that the increased stability and altered binding affinity led to carfilzomib-induced increase in p53 target gene expression of PAD4, which promoted NET formation. Since neutrophils do not survive freezing in liquid nitrogen and because we could not identify a living patient with a similar mutation from our patient cohorts, we cannot prove this causal relationship. Therefore, the here reported relation referenced in the title as one clonal hematopoiesis of indeterminate potential (CHIP) that may be responsible for three pathologies, namely MM, MDS and carfilzomib-induced lung-induced injury remains speculative in nature. Because effects of steroids on immune cells are broad, it is likely that additional cells not studied herein have been affected and we recommend to carefully draw conclusions. Despite these limitation, this case may contribute to the growing number of clinical pathologies associated with CHIP.<sup>15</sup>

In conclusion, we present the first clinic-mechanistical evidence that steroid-responsive DILI with GGO following PI is associated with neutrophilic lung infiltrates and increased NET formation. This may also be relevant for ARDS with neutrophil infiltration sometimes lacking causal explanation. Furthermore, we correlate DILI-onset with a CHIP clone emphasizing the significance of molecular diagnostics and its impact on clinical conditions.

## Authors

Julia Katharina Scholz,<sup>1,2\*</sup> Lena Stabel,<sup>1,2\*</sup> Nora Rebecca Schwingen,<sup>1,2</sup> Jasmin Knopf,<sup>3,4,5</sup> Anna-Sophie Flatt,<sup>1,2</sup> Tobias Bäuerle,<sup>6</sup> Stefan Krause,<sup>1,2</sup> Heidi Waibel,<sup>1,2</sup> Moritz Leppkes,<sup>7</sup> K. Martin Kortüm,<sup>8,9</sup> Hermann Einsele,<sup>8,9</sup> Andreas Mackensen,<sup>1,2</sup> Martin Herrmann,<sup>3,4,5#</sup>

Simon Völkl<sup>1,2#</sup> and Fand Fabian Müller<sup>1,2#</sup>

<sup>1</sup>Department of Internal Medicine 5 - Hematology and Oncology, Friedrich-Alexander-Universität Erlangen-Nürnberg (FAU) and Uniklinik Erlangen, Erlangen; <sup>2</sup>Bavarian Cancer Research Center (BZKF), Erlangen, Germany; <sup>3</sup>Department of Internal Medicine 3 - Rheumatology and Immunology, Friedrich-Alexander-Universität Erlangen-Nürnberg (FAU) and Uniklinik Erlangen, Erlangen; <sup>4</sup>Department of Pediatric Surgery, University Medical Center Mannheim, Heidelberg University, Mannheim; <sup>5</sup>Deutsches Zentrum für Immuntherapie, Friedrich-Alexander-Universität Erlangen-Nürnberg (FAU) and Uniklinik Erlangen, Erlangen; <sup>6</sup>Department of Diagnostic and Interventional Radiology, Universitätsmedizin Mainz; <sup>7</sup>Department of Internal Medicine 1, Friedrich-Alexander-Universität Erlangen-Nürnberg (FAU) and Uniklinik Erlangen, Erlangen; <sup>8</sup>Medizinische Klinik und Poliklinik II, Uniklinikum Würzburg, Würzburg and <sup>9</sup>Bavarian Cancer Research Center (BZKF), partner site Würzburg, Germany

\*JKS and LS contributed equally as first authors.

#MH, SV and FM contributed equally as senior authors.

Correspondence:

F. MÜLLER - fabian.mueller@uk-erlangen.de

<https://doi.org/10.3324/haematol.2024.286596>

Received: October 9, 2024.

Accepted: February 5, 2025.

Early view: February 13, 2025.

©2025 Ferrata Storti Foundation

Published under a CC BY-NC license 

## Disclosures

JKS received travel support from Beigene, AbbVie, Janssen and Novartis. LS received travel support from Beigene and AbbVie. MK reports grant funding and personal fees from AbbVie, Bristol-Myers Squibb, GSK, Pfizer, Takeda, Menarini-Stemline, Janssen-Cilag and Sanofi. HE has consulted for BMS/Celgene, Janssen, Amgen, Takeda, Sanofi, GSK and Novartis; he has received research funding from BMS/Celgene, Janssen, Amgen, GSK and Sanofi; discloses honoraria from BMS/Celgene, Janssen, Amgen, Takeda, Sanofi, GSK, Novartis and travel support from BMS/Celgene, Janssen, Amgen, Takeda, Novartis and Sanofi. AM has consulted and/or provided lectures for Gilead/KITE, Novartis, BMS/Celgene and Miltenyi Biomedicine; and was part of the scientific advisory board of Miltenyi Biomedicine, Ixaka, Novartis, BMS/Celgene, Gilead/KITE, Kyverna and Century Therapeutics. MH is a shareholder and adviser of Neutrolis, Inc., Cambridge, MA, USA. FM was part of the advisory board of ArgoBIO, AstraZeneca, BMS, CRISPR Therapeutics, EcoR1, Janssen, Kite/Gilead, Miltenyi, Novartis and Sobi; contributed to the Speakers Bureau of AstraZeneca, AbbVie, Beigene, BMS, Incyte; Janssen, Kite/Gilead, Miltenyi, MSD, Novartis, Pfizer, Sobi and Takeda; and received research funding of MedImmune/AstraZeneca, BMS and Kite/Gilead.



All other authors have no conflicts of interest to disclose.

### Contributions

FM, HW, SK and AM designed treatments and analyses. MH and SV designed biologic studies and analyzed data. JKS, LS and A-SF monitored the patient. JKS, LS, HE, MK, TB and ML collected clinical data. NRS and JK conducted experiments and analyzed data. JKS, LS and FM wrote the manuscript.

### Acknowledgments

This publication is dedicated to the patient and his wife who together celebrated every moment they gained through the many treatment lines of his multiple myeloma. We are grateful for their openness and willingness to support science with the goal of helping the coming patients. He will be missed. We want to thank Heike Ebner for excellent sample management and Florentine Schonath (Core Unit Cell Sorting and Immunomonitoring Erlangen), Dorothea Gebhardt, Lina Meretuk, Denise Schellmann, Lena Tarantik and Luisa Albert for excellent technical assistance. Molecular genetics data on native bone marrow samples and cell fractions enriched or depleted in CD138-positive cells via magnetically

assisted cell sorting (MACS) of bone marrow material was provided by the Munich Leukemia Laboratory (MLL).

### Funding

This research was supported by the NOTICE clinician scientist program of the Deutsche Forschungsgemeinschaft grant number 493624887 (Clinician Scientist Program NOTICE) (to JKS), the “Bayerisches Zentrum für Krebsforschung” grant number TLG-22 (to FM), the Deutsche Krebshilfe grant number 70116123 (to FM), the Bundesministerium für Bildung und Forschung (BMBF) advanced clinician scientist program iIMMUNE grant number 01EO2105 (to FM), the Interdisziplinäre Zentrum für Klinische Forschung (IZKF) project grant number D43 (to SV), and the European Commission 861878 “NeutroCure” (to MH).

### Data-sharing statement

The data supporting the findings of this study are available upon request via email to the corresponding author within the data protection constraints in the written informed consent signed by the study participant.

## References

1. Skeoch S, Weatherley N, Swift AJ, et al. Drug-induced interstitial lung disease: a systematic review. *J Clin Med*. 2018;7(10):356.
2. Leonardo-Sousa C, Carvalho AN, Guedes RA, et al. Revisiting proteasome inhibitors: molecular underpinnings of their development, mechanisms of resistance and strategies to overcome anti-cancer drug resistance. *Molecules*. 2022;27(7):2201.
3. Lataifeh AR, Nusair A. Fatal pulmonary toxicity due to carfilzomib (Kyprolis™). *J Oncol Pharm Pract*. 2016;22(5):720-724.
4. Bhagavath A, Geyer A. Carfilzomib pulmonary toxicity. *Chest*. 2016;150(4):492a.
5. Kwong YL. Fatal pulmonary hemorrhage after carfilzomib treatment in multiple myeloma. *Ann Hematol*. 2015;94(8):1425-1426.
6. Saglam B, Kalyon H, Ozbalak M, et al. Bortezomib induced pulmonary toxicity: a case report and review of the literature. *Am J Blood Res*. 2020;10(6):407-415.
7. Dhakal A, Belur AA, Chandra AB. Bortezomib induced pulmonary toxicity. *Blood*. 2014;124(21):5731-5731.
8. Davidson KR, Ha DM, Schwarz MI, Chan ED. Bronchoalveolar lavage as a diagnostic procedure: a review of known cellular and molecular findings in various lung diseases. *J Thorac Dis*. 2020;12(9):4991-5019.
9. Leppkes M, Knopf J, Naschberger E, et al. Vascular occlusion by neutrophil extracellular traps in COVID-19. *EBioMedicine*. 2020;58:102925.
10. Thiam HR, Wong SL, Wagner DD, Waterman CM. Cellular mechanisms of NETosis. *Annu Rev Cell Dev Biol*. 2020;36:191-218.
11. Wang Y, Li M, Stadler S, et al. Histone hypercitrullination mediates chromatin decondensation and neutrophil extracellular trap formation. *J Cell Biol*. 2009;184(2):205-213.
12. White KA, Ruiz DG, Szpiech ZA, et al. Cancer-associated arginine-to-histidine mutations confer a gain in pH sensing to mutant proteins. *Sci Signal*. 2017;10(495):eeam9931.
13. Gully CP, Velazquez-Torres G, Shin JH, et al. Aurora B kinase phosphorylates and instigates degradation of p53. *Proc Natl Acad Sci U S A*. 2012;109(24):E1513-1522.
14. Tanikawa C, Ueda K, Nakagawa H, Yoshida N, Nakamura Y, Matsuda K. Regulation of protein Citrullination through p53/PADI4 network in DNA damage response. *Cancer Res*. 2009;69(22):8761-8769.
15. Singh J, Li N, Ashrafi E, et al. Clonal hematopoiesis of indeterminate potential as a prognostic factor: a systematic review and meta-analysis. *Blood Adv*. 2024;8(14):3771-3784.